Optical Spin Orientation of a Single Manganese Atom in a Semiconductor Quantum Dot Using Quasiresonant Photoexcitation

C. Le Gall, L. Besombes,* H. Boukari, R. Kolodka, J. Cibert, and H. Mariette

CEA-CNRS group "Nanophysique et Semiconducteurs," Institut Néel, CNRS and Université Joseph Fourier, 25 Avenue des Martyrs, 38042 Grenoble, France

(Received 13 November 2008; published 24 March 2009)

An optical spin orientation is achieved for a Mn atom localized in a semiconductor quantum dot using quasiresonant excitation at zero magnetic field. Optically created spin-polarized carriers generate an energy splitting of the Mn spin and enable magnetic moment orientation controlled by the photon helicity and energy. The dynamics and the magnetic field dependence of the optical pumping mechanism show that the spin lifetime of an isolated Mn atom at zero magnetic field is controlled by a magnetic anisotropy induced by the built-in strain in the quantum dots.

DOI: 10.1103/PhysRevLett.102.127402 PACS numbers: 78.67.Hc, 75.75.+a, 78.55.Et

Controlling the interaction between spin-polarized carriers and magnetic atoms is of fundamental interest to understand the mechanism of spin transfer. Spin transfer could lead to the development of devices in which the spin state of magnetic atoms is controlled by the injection of a spin-polarized current and not by an external magnetic field, as in conventional magnetic memories. Information storage on a single magnetic atom would be the ultimate limit in the miniaturization of these memories. Dilute magnetic semiconductor systems combining semiconductor heterostructures and the magnetic properties of Mn dopant are good candidates for these devices [1]. In a dilute magnetic semiconductor, optically injected spin-polarized carriers couple with localized Mn spins allowing, e.g., photo-induced magnetization to be achieved [2,3]. It has been known for years that, in the absence of carriers and under a magnetic field, highly dilute ensembles of Mn present a spin relaxation time in the millisecond range [4]. However, the dynamics of such ensembles can be much faster at zero field [5]. In addition, very little is known about the zero field dynamics of a single Mn spin, and the optical spin orientation of a single magnetic atom in a solid state environment is still a challenge [6].

In this Letter, we present a new way to optically address the spin of a single Mn atom localized in a quantum dot (QD): the injection of spin-polarized carriers and spin selective optical excitation is used to prepare a nonequilibrium Mn spin distribution without any applied magnetic field. Photoluminescence (PL) transients recorded when switching the circular polarization of the excitation reflect the dynamics of this optical orientation mechanism. The magnetic field dependence of the optical pumping efficiency reveals the influence of the Mn fine structure on the spin dynamics: the strain induced magnetic anisotropy of the Mn spin slows down the relaxation at zero magnetic field. We show that the Mn spin distribution prepared by optical pumping is fully conserved for a few microseconds.

Growth and optical addressing of QDs containing a single Mn atom were achieved recently [7–9]. The static properties of these systems are now well understood: when a Mn atom is included in a II-VI QD, the spin of the optically created electron-hole pair interacts with the five d electrons of the Mn (total spin $S = 5/2$). This leads to a splitting of the once simple PL spectrum of a QD into six $(2S + 1)$ components [Fig. 1(a)]. This splitting results from the spin structure of the confined holes which are quantized along the QDs' growth axis with their spin component taking only the values $J_z = \pm 3/2$ [10]. The hole-Mn exchange interaction reduces to an Ising term $J_z S_z$ and shifts the PL energy according to the relative projection of the Mn and hole spins [11]. The intensity of each line reflects the probability for the Mn to be in one of its six spin components, and it is a probe of the Mn spin at the moment the exciton recombines [12].

To optically pump the Mn spin, Mn-doped QDs were quasiresonantly excited with a tunable continuous wave (cw) dye laser. In order to record the spin transients, the linear polarization of the excitation laser was modulated between two orthogonal states by switching an electro-optic modulator with a rise time of 5 ns, and converted to circular polarization with a quarter-wave plate. Trains of resonant light with variable duration were generated from the cw laser using acousto-optical modulators with a switching time of 10 ns. The circularly polarized collected light was dispersed by a 1 m double monochromator before being detected by a fast avalanche photodiode in conjunction with a time correlated photon counting unit with an overall time resolution ~50 ps.

Figures 1 and 2 summarize the main features of the time-resolved optical orientation experiment. The PL of the exciton-Mn (X-Mn) system was excited in one of the excited states of the X-Mn complex [top of Fig. 1(a)] [13]; the PL intensity was measured in circular polarization. Then the relative intensity of the six lines dramatically depends on the state selected for the excitation [bottom of Fig. 1(a)]: as each line corresponds to one value of the Mn spin projection S_z, that shows that the whole process creates a nonequilibrium distribution of the X-Mn

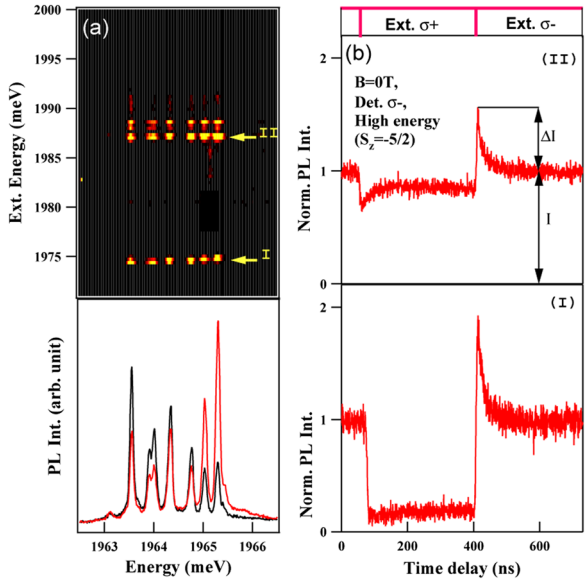

FIG. 1 (color online). (a) PL and PL excitation of a Mn-doped QD at $B = 0$ T and $T = 5$ K. The PL is detected in circular polarization under an alternate σ^- and σ^+ excitation at two different wavelengths into the same set of excited states: 1987.0 meV (black line) and 1987.4 meV [gray (red) line]. (b) PL transient under polarization switching at $B = 0$ T. The PL is detected on the high energy line of X-Mn in σ^- polarization (Mn spin $S_z = -5/2$). Transient (I) [(II)] was observed under resonant excitation at 1975 meV (1987 meV).

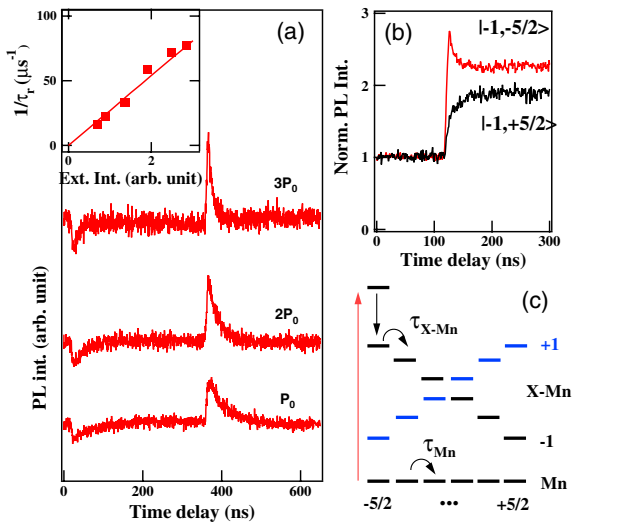

FIG. 2 (color online). (a) PL transients at different values of the excitation power. Inset: power dependence of the inverse response time τ_r, taken at the $1/e$ point of the spin-related transient. (b) PL transients recorded in σ^- polarization on the high ($S_z = -5/2$) and low ($S_z = +5/2$) energy line of the X-Mn complex. (c) Simplified level diagram of a Mn-doped QD, as a function of Mn spin (X-Mn: bright exciton-Mn).

spin states. Under these conditions, switching the circular polarization of the excitation produces a change of the PL intensity [Fig. 1(b)] with two transients: first an abrupt one, reflecting the population change of the spin-polarized excitons; then a slower transient with opposite signs on the two extreme PL lines [i.e., when monitoring the Mn spin states $S_z = +5/2$ or $S_z = -5/2$, Fig. 2(b)], and a characteristic time which is inversely proportional to the pump intensity [Fig. 2(a)]. This is the signature of an optical pumping process which realizes a spin orientation of the Mn atom. We first discuss the details of this process, then use it to study the spin dynamics of the single Mn in the QD.

The relevant sublevels of X-Mn and Mn are schematized in Fig. 2(c). For the sake of simplicity, we omit the dark exciton states which should be included for a quantitative analysis and consider that the dynamics can be described by two spin relaxation times, one for the Mn alone τ_{Mn} and one within the X-Mn complex $\tau_{X\text{-Mn}}$ [12,14]. When exciting one of the excited states of the QD, two mechanisms are expected to contribute to the observed spin orientation: first the selective excitation of the QD shows a strong dependence on the Mn spin state [13], and second the relaxation of the Mn spin within the X-Mn system is driven by the interaction with the spin-polarized carriers which have been injected.

Under spin selective excitation, the spin relaxation of X-Mn tends to empty the spin state of the Mn, which gives rise to an absorption maximum [14]. Within the X-Mn system, $\tau_{X\text{-Mn}}$ is influenced by carrier-phonon, carrier-nuclei, and exchange interactions affecting the exciton [14–16]. The off-diagonal terms of the sp-d exchange interaction [11,12] allow simultaneous spin-flips of carrier and Mn spins, and a spin transfer from the injected carriers to the Mn is made possible. Alternatively, a spin-flip of the Mn in the exchange field of the exciton could also contribute to a Mn spin orientation.

If $\tau_{X\text{-Mn}}$ is shorter than τ_{Mn}, a dynamic spin orientation of the Mn can be performed. Under injection of spin-polarized carriers, relaxation processes tend to antialign the Mn spin with the X exchange field to reach a thermal equilibrium on the X-Mn levels [14]. Hence, optical pumping with σ^- photons, for instance, tends to decrease the population of the spin state $S_z = -5/2$ and decrease that of $S_z = +5/2$, as observed in Fig. 2(b).

Both mechanisms, absorption selectivity and spin injection, depend on the structure of the excited states, resulting in a pumping signal which depends on the excitation energy (Fig. 1). An efficient pumping of the Mn spin can be performed within a few tens of ns, showing that at $B = 0$ T the spin relaxation time of the Mn alone is long enough compared to the X-Mn dynamics.

Having established a method to prepare Mn spins, we performed pump-probe experiments to observe how the Mn polarization is conserved (Fig. 3). We prepare a non-equilibrium distribution of the Mn spin with a $\sigma^{\pm}$ pulse. The pump laser is then switched off, and switched on again after a dark time t_{dark}. We observe no transient if the laser is switched on with the same polarization, and a transient of constant intensity when the polarization has been changed,

whatever the value of t_{dark} up to the μs range. This demonstrates that in the absence of charge fluctuations [i.e., neutral QD (see inset of Fig. 3)] the prepared Mn spin is conserved over μs. The injection of unpolarized high energy carriers in the vicinity or in the QD significantly increases the Mn spin relaxation rate [12]. This is illustrated in Fig. 3(c): the PL transient is recovered when free carriers have been injected during the dark time with a second nonresonant laser, thus erasing the single spin memory.

More information can be obtained from the magnetic field dependence of the optical pumping signal. For an isotropic Mn spin, the decoherence of the precessing spin in a transverse field would give rise to a Hanle depolarization curve with a Lorentzian shape and a width proportional to $1/T_2$ [6]. In the present case, a magnetic field in the Faraday configuration (B_z) does not change significantly the PL transients [Fig. 4(b)]: a weak increase of the spin orientation efficiency is observed as soon as a field of a few mT is applied; above that, the pumping efficiency remains constant. By contrast, an in-plane field (B_x) induces coherent precession of the Mn spin away from the optical axis (= QDs' growth axis), so that the average spin polarization, and therefore the amplitude of the optical pumping signal, decay [Fig. 4(a)].

It is known from electron paramagnetic resonance spectroscopy that the ground state of Mn^{2+} presents a fine structure [17]. In a cubic crystal, it results from a strong hyperfine coupling with the Mn nuclear spin, $A\,\mathbf{I}\cdot\mathbf{S}$ (with $I = 5/2$ and $A \approx 0.7$ μeV), and the crystal field. In addition, in epitaxial structures, built-in strains due to the lattice mismatch induce a magnetic anisotropy with an easy axis along the QD axis; it scales as $D_0 S_z^2$, with D_0 proportional to the tetragonal strain [17]. The resulting fine structure under a magnetic field applied in-plane or out-of-plane is shown in Fig. 5(a). At zero field, the Mn electronic spin is quantized along the growth axis, and the different electronic spin doublets are separated by an energy proportional to D_0. Each level is further split into six lines by the hyperfine coupling.

This structure controls the Mn spin dynamics at zero or weak magnetic field. At zero field, in the absence of anisotropy, the precession of the electronic spin of Mn in its own hyperfine field should erase any information stored on the electronic spin [5]. In the presence of anisotropy, the precession of the Mn spin in the nuclear field is blocked even at $B = 0$ T. This is shown in Fig. 5(b), where we plot the evolution of the density matrix element $\rho_{5/2}(t)$, calculated for the electronic + nuclear spin system of a single Mn ion using the master equation $d\rho_S(t)/dt = -(i/\hbar)[\mathcal{H}_{Mn}, \rho_S(t)]$ (no relaxation) with the initial condition $\rho_{5/2}(0) = 1$ ($S_z = +5/2$ and random nuclear spin I_z). With $D_0 = 0$, the coherent evolution of the electronic spin in the nuclear field erases the orientation of the electronic spin in a few 100 ps. With a D_0 of a few μeV, this free precession is blocked, and the Mn spin can be conserved for a long time, in agreement with Fig. 3. In particular, it is conserved during the time interval between the injection of two consecutive excitons, allowing the optical pumping mechanism to take place.

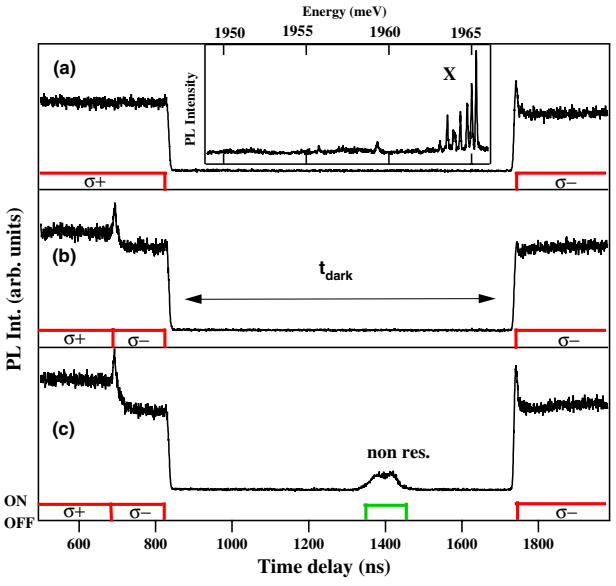

FIG. 3 (color online). PL transients recorded under the optical polarization sequence displayed at the bottom of each plot. The prepared Mn spin is conserved during t_{dark}: in (a) and (b), a transient is observed only for a different helicity of the pump and the probe. The injection of carriers with a nonresonant excitation (514 nm) forces the relaxation of the Mn spin (c). Inset: PL obtained under the resonant excitation condition used in the optical pumping measurements.

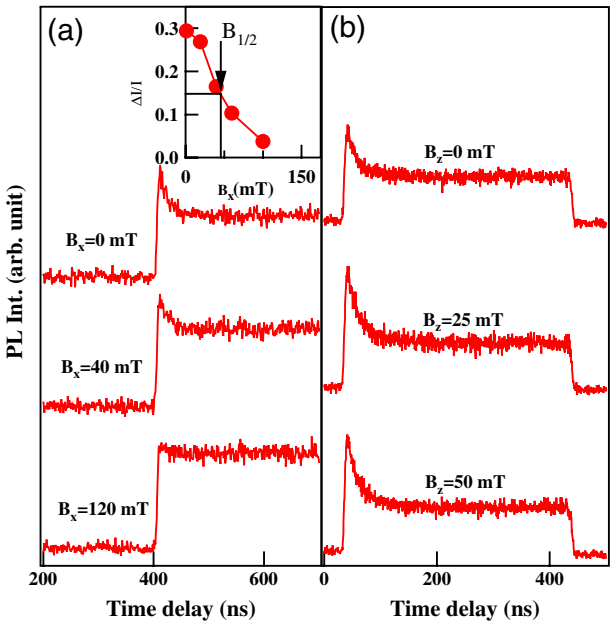

FIG. 4 (color online). Mn spin transient as a function of a magnetic field applied in-plane (a) and out-of-plane (b). Inset: transverse field dependence of the transient amplitude $\Delta I/I$ (see Fig. 1). $B_{1/2}$ is the half width at half maximum.

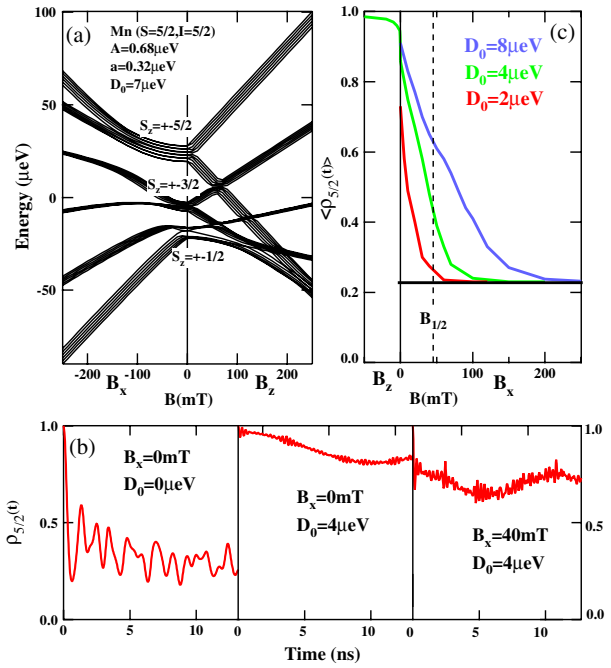

FIG. 5 (color online). (a) Magnetic field dependence of the fine structure of the Mn spin with out-of-plane (right) and in-plane (left) fields, calculated with $A = 0.68$ μeV, $D_0 = 7$ μeV, and a crystal field parameter $a = 0.32$ μeV. (b) Time evolution of $\rho_{+5/2}(t)$ calculated for different values of D_0 and B_x with $\rho_{+5/2}(0) = 1$. (c) Time average value of $\rho_{+5/2}(t)$ versus B_x for different values of D_0 ($T_2 = \infty$). The $B_{1/2}$ found experimentally is indicated with a dotted line.

The magnetic anisotropy also blocks the Mn spin precession in a weak transverse field. Then the transverse field dependence of the optical pumping efficiency is controlled both by the anisotropy D_0 and the coherence time T_2. A dephasing time $T_2^* \simeq 1$ ns has been measured in an ensemble of CdMn(2%)Se QDs [18]; a longer decoherence time T_2 is expected for a single isolated Mn spin. For $T_2 \geq 1$ ns, the influence of the decoherence on the width of the depolarization curve is smaller than 4 mT, and its contribution to the experimental curve [Fig. 3(a)] can be neglected. Hence, in order to estimate D_0, we take again $T_2 = \infty$ to calculate the density matrix element $\rho_{5/2}(t)$ for $\rho_{5/2}(0) = 1$, assuming various values of D_0.

Figure 5(c) displays the field dependence of the time-averaged value of $\rho_{5/2}(t)$ [$\langle\rho_{5/2}(t)\rangle$]. This quantity describes the probability for the state $S_z = +5/2$ to be conserved after the recombination of an exciton, as the electronic Mn spin evolves in the hyperfine field, the crystal field, and the applied magnetic field. A decrease in this spin conservation progressively destroys the cumulative process controlling the optical pumping mechanism. For a free precessing spin, $\langle\rho_{5/2}(t)\rangle \approx 0.24$ as soon as a transverse field is applied and the depolarization is controlled by T_2 [6]. In the presence of anisotropy, the Mn spin does not precess at weak field, and the Mn spin state is partially conserved [Fig. 5(b)]. When the transverse field is strong enough to overcome the magnetic anisotropy ($g_{\mathrm{Mn}}\mu_B B_x \gg D_0$), $\langle\rho_{5/2}(t)\rangle$ reaches the expected value for a coherently precessing spin. This decrease of $\langle\rho_{5/2}(t)\rangle$ gives rise to a field-induced depolarization curve depending on D_0. A half-height field $B_{1/2} \simeq 45$ mT, as observed experimentally in Fig. 4(b), is obtained for $D_0 \approx 6$ μeV. As a value $D_0 \approx 12$ μeV is expected for CdTe coherently grown on ZnTe [17]; this is consistent with the presence of a CdZnTe alloy or a partial relaxation of the mismatch strain at the Mn location.

A large magnetic anisotropy which blocks the Mn spin relaxation also explains the weak influence of an out-of-plane field. Nevertheless, the Zeeman splitting cancels the nondiagonal coupling induced by the crystal field and improves the Mn spin conservation [left part in Fig. 5(c)], thus accounting for the increase of the optical pumping efficiency in weak field [Fig. 4(b)].

To conclude, our results demonstrate the optical spin orientation of a single magnetic atom in a semiconductor host. Optical excitation of an individual Mn-doped QD with circularly polarized photons can be used to prepare a nonequilibrium distribution of the Mn spin without any applied magnetic field. Resonant excitation of the QD ground state should permit a higher fidelity preparation of the Mn spin. It should then be possible to initialize a Mn spin, manipulate it on a μs time scale with microwave excitation, and reliably read the final state.

Supported by ANR contracts MOMES and CoSin.

*lucien.besombes@grenoble.cnrs.fr

[1] J. Fernandez-Rossier and R. Aguardo, Phys. Rev. Lett. **98**, 106805 (2007).
[2] H. Krenn *et al.*, Phys. Rev. B **39**, 10918 (1989).
[3] A. V. Koudinov *et al.*, Phys. Solid State **45**, 1360 (2003).
[4] T. Dietl *et al.*, Phys. Rev. Lett. **74**, 474 (1995).
[5] M. Goryca *et al.*, Phys. Rev. Lett. **102**, 046408 (2009).
[6] R. C. Myers *et al.*, Nature Mater. **7**, 203 (2008).
[7] L. Besombes *et al.*, Phys. Rev. Lett. **93**, 207403 (2004).
[8] L. Maingault *et al.*, Appl. Phys. Lett. **89**, 193 109 (2006).
[9] A. Kudelski *et al.*, Phys. Rev. Lett. **99**, 247209 (2007).
[10] Y. Léger *et al.*, Phys. Rev. B **72**, 241309(R) (2005).
[11] Y. Léger *et al.*, Phys. Rev. B **76**, 045331 (2007).
[12] L. Besombes *et al.*, Phys. Rev. B **78**, 125324 (2008).
[13] M. M. Glazov *et al.*, Phys. Rev. B **75**, 205313 (2007).
[14] A. O. Govorov and A. V. Kalameitsev, Phys. Rev. B **71**, 035338 (2005).
[15] D. H. Feng, I. A. Akimov, and F. Henneberger, Phys. Rev. Lett. **99**, 036604 (2007).
[16] L. M. Woods, T. L. Reinecke, and R. Kotlyar, Phys. Rev. B **69**, 125330 (2004).
[17] M. Qazzaz *et al.*, Solid State Commun. **96**, 405 (1995).
[18] M. Scheibner *et al.*, Phys. Rev. B **73**, 081308(R) (2006).